

Friction Dynamics of Geckolike Materials

Jonathan B. Puthoff¹

¹California State Polytechnic University, Pomona, 3801 West Temple Avenue, Pomona, CA 91768, U.S.A.

ABSTRACT

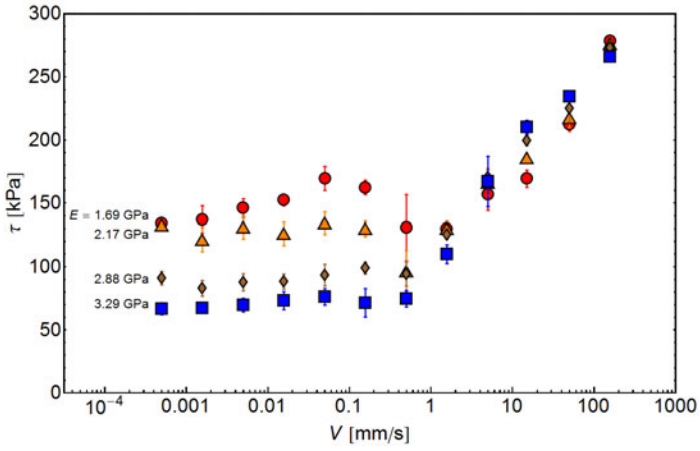
The interface between the adhesive toes of geckos and a substrate consists of an array of regularly sized, densely packed, and elastically coupled nanoscopic contacts. The velocity-dependent friction exhibited by this system hints at a convolution of various material and structural effects. We explore the dynamics of frictional sliding in these materials using models based on arrays of coupled masses driven by external forces that can become pinned and unpinned to a potential energy landscape. The model system is driven at normalized velocities spanning 6 orders of magnitude, and the output of this model captures both the low- V and high- V behavior of the actual gecko materials. We explore modifications to the essential model that incorporate features more representative of the structure and behavior of the natural gecko system. These results have implications in the design of materials with custom frictional properties.

INTRODUCTION

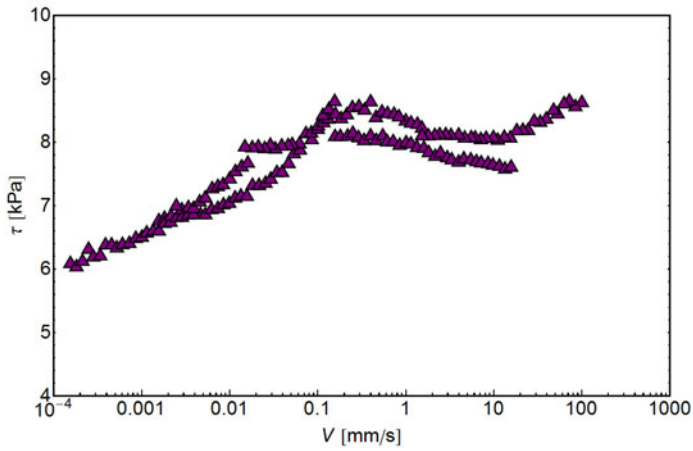
The gecko adhesion system provides these animals with an impressive suite of capabilities during climbing, such as robust attachment, easy release, and tolerance to contamination [1]. The system is based on the microscale hair-like protrusions on the underside of the geckos' toes; these branched keratinous structures, when suitably deployed, securely attach the animal to the underlying surface with weak intermolecular forces acting at the nanoscopic contacts. The mechanisms underpinning this adaptation have considerable relevance to the evolution and biomechanics communities, but a close study of these physical principles can inform the development of synthetic adhesives as well as new theories of tribology [2].

Recent measurements of the dynamic friction produced by natural gecko setal arrays and synthetic geckolike adhesives [3, 4] require an explanation in terms of fundamental tribological principles. Dynamic friction (or rate-dependent friction) is the force response of a system of two bodies in contact moving with some relative velocity V . Traditional teaching on the topic of friction implicitly recognizes this rate dependence, categorizing the friction force as either "static" or "kinetic," but in general friction forces can vary continuously with V . V -dependent stresses (i.e., forces normalized to specimen areas) produced by geckolike materials, both natural and synthetic, are shown in Figure 1. The curves show different regimes of behavior associated with different domains of V . Previous work [4] attempted to explain these effects using a product of functions representing distinct rate and state behaviors of an ensemble of contacts. These models are unsatisfying since the rate and state functions are somewhat arbitrary.

In this paper, I discuss the origins of these different force regimes and illustrate how they can arise from the dynamics of a system of externally-driven coupled nanoscale contacts. These types of models [5, 6] have been developed to treat friction generally, but the gecko material offers an opportunity to test them against systems which possibly conform better to the underlying assumptions, namely uniformly sized and spaced nanoscopic contacts. A better



(a)



(b)

Figure 1. Dynamic friction in (a) natural and (b) synthetic geckolike materials, after [4]. Friction stress τ depends on the imposed velocity V . Different $\tau(V)$ behaviors are associated with different velocity regimes. In the case of the natural material, different values of elastic modulus produce different low- V behavior.

understanding of this model and the connections between model properties and the behavior of real materials systems would simultaneously explicate design principles for synthetic materials and advance the science of friction between extended bodies across numerous asperities.

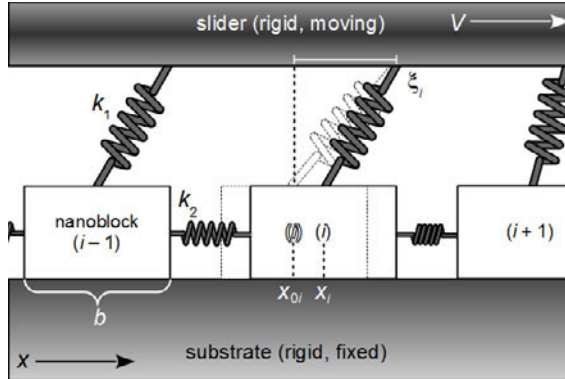


Figure 2. Diagram of the 1D coupled sliding nanoblock array and defining model parameters.

THEORY

During frictional sliding in natural and synthetic geckolike adhesives, individual contacts may exist in a number of states: pinned to the surface by some confining interaction potential or in the process of slipping across the surface. Additionally, the state of the contacts may change with changes in the states of neighboring contacts. A picture of a simplified model of the subdivided interface is shown in Figure 2. This system consists of N nanoscopic contact volumes, or “nanoblocks,” of size b and mass m whose positions are labelled by the components of the vector x_i . The nanoblocks are coupled elastically to body at large by idealized springs of stiffness k_1 at the vector of attachment points ξ_i . The blocks are also coupled to each other by springs of stiffness k_2 . The slider is driven at velocity V .

The equation of motion for block i is

$$m(d^2x_i / dt^2) + c(dx_i / dt) - k_2(x_{i+1} + x_{i-1} - 2x_i) = k_1(\xi_i - x_i), \quad (1)$$

where c is a damping coefficient that reflects the interfacial dissipation in a sliding nanoblock proportional to its velocity $v_i = dx_i / dt$. The forces that act on the nanoblocks across the interface are represented by a set of rules:

- 1) A nanoblock with $v_i = 0$ is pinned to the substrate until the elastic forces f_i acting on it exceed a threshold force f_0 (or stress $\tau_0 = f_0 / b^2$); and
- 2) a nanoblock whose velocity drops to zero under the influence of the combined elastic and damping forces becomes repinned with the driving force $k_1(\xi_i - x_i)$ relaxing to 0.

Because the interfacial potential implied by these rules has no simple representation and the goal is to simulate a large number of contacts, a numerical approach with discrete time steps is required. Additionally, I solve the system using units that nondimensionalize the problem. Time is measured in units of $(m/k_2)^{1/2}$ and position in units of f_0/k_2 . The damping ratio ζ is defined as

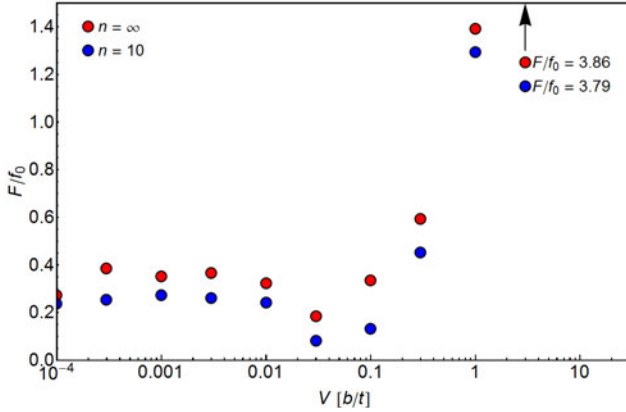


Figure 3. Normalized average nanoblock force vs. slider velocity. The data for $V = 3$ are off of the scale; plotting the data this way reveals more clearly the qualitative shift in behavior at $V^* \approx 0.03$. At velocities less than V^* , the system is essentially static; the blocks are predominately pinned. When the degree of coupling n is reduced, the $F/f_0(V)$ curves shift to lower force levels, seemingly uniformly at all V .

$c/2(mk_2)^{1/2}$. Taking these steps transforms Eq. 1 into

$$(d^2x_i / dt^2) + 2\zeta(dx_i / dt) + (k_2 / k_1)(x_{i+1} + x_{i-1} - 2x_i) + x_i - \xi_i = 0. \quad (2)$$

My solutions to Eq. 2 incorporated $N = 100$ blocks and employed $m = 1$, $k_1 = k_2 = 1$, and $c = 1$. Additionally, $b = 1$ and $f_0 = 1$. The initial block driving forces $x_i - \xi_i$ were randomized and uniformly distributed between 0 and 1. The blocks have size $b = f_0/k_2$, and I generated solutions for driving velocities $0.00003 b/t \leq V \leq 3 b/t$. The solutions – i.e., block positions and velocities at each solver step – were generated using a custom MATLAB procedure (incorporating the ode45 solver) for $0 \leq t \leq 2000$. I calculated the net block forces F_i at each step, as well as the descriptive parameter $h(t)$, defined as the fraction of blocks with $v_i > 0$ at time t .

I also generated a second set of solutions with the same parameters as above but an additional modification: the degree of coupling between the blocks was reduced. In the natural gecko material, the hairs are bundled hierarchically. This means that adjacent contacts might only be elastically coupled several levels removed in the hierarchy. Since the pathway for elastic energy return between these otherwise adjacent contacts is so torturous, the contacts are effectively decoupled. The degree of coupling n is the number of nanoblocks that are serially coupled to each other but uncoupled from the next n blocks. I.e., $k_2(x_{i+1} - x_i) = 0$ if $i \bmod n = 0$. This additional set of V -dependent simulations took $n = 10$.

DISCUSSION

The resulting F and h data vary continuously with V and possess a number of distinguishing features. Figure 3 shows the average normalized force F/f_0 on the blocks during the simulation

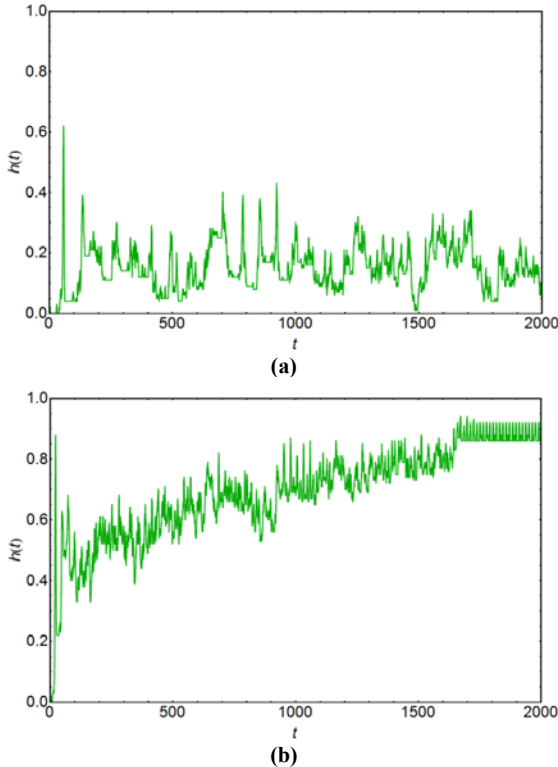


Figure 3. (a) Creeplike ($V = 0.01$) and **(b)** transitional ($V = 0.0$) system behaviors reflected in the parameter h . The low- V data indicate a system that is pinned, overall, and essentially static. When driven near the critical velocity V^* , the initially pinned system gradually transitions to a state where the blocks move freely. When the block move freely

against the driving velocity for both the fully coupled case and $n = 10$. In both cases, the force data are approximately constant at low V , drop slightly somewhere in the range $0.01 \leq V \leq 0.1$, then rise rapidly. This transition corresponds to a qualitative change in behavior near some characteristic velocity I call V^* . A comparison of the F/f_0 vs. V curves for the two different n treatments indicate a reduction in friction force levels. This reduction is presumably the result of removing some elastic elements from the system. V^* appears to be unchanged with n in this case.

Figure 4 shows the function $h(t)$ for driving velocities of 0.01 and 0.03 b/t .; these data capture the nature of the shift in system behavior at V^* . At $V < V^*$ the number of blocks in motion at any given time is typically small: $h < 0.15$. The behavior in this region of the force vs.

velocity curve is creeplike, since the system behavior is defined by the jumping motion and subsequent relaxation of individual nanoblocks or clusters of blocks. Although highly correlated motions of clusters of blocks appear as spikes in $h(t)$ that rise as high as 0.5, the overall state of the system is essentially statically pinned.

Near V^* , the collective motion of large numbers of blocks occurs, and the system evolves toward a state where block motions are continuous with little repinning. The nanoblocks are essentially advected along with the rest of the body at approximately the imposed velocity V . This change in dynamics is reflected in the force data; the elastic stresses decrease as more blocks become free, though the dissipation (via the damping ζ) is still too small to make up the difference. As V increases further, the dissipative forces dominate the system behavior.

The results of these simulations have a striking resemblance to those for the natural gecko material in Figure 1(a). (The fact that the real experiments are essentially 2D while the simulations are 1D can be reconciled if we think of the simulations as providing the dynamic friction forces on a per-unit-width basis.) The flat, creeplike regions at low V are congruent in both the real and simulated force data, as are the high- V regions where the forces are rate sensitive. The weaker overall coupling introduced by the choice of $n = 10$ does not appear to have a readily interpretable meaning in the real data, indicating there are effects that are unaccounted for in current modeling efforts.

CONCLUSIONS

A physical model of friction at a sliding interface based on coupled masses driven at a velocity V has the features required to explain the performance of the regular, hierarchical gecko attachment system. Because the masses can become individually pinned to the substrate by static friction forces, there is an interaction between the rate at which the system is driven and the overall relaxation rate of the depinning and repinning contacts; this interaction produces the rich system behavior observed across a logarithmic span of imposed rates. When a degree of decoupling (representing coupling at a higher hierarchical level) is introduced, the static and dynamic friction forces are altered significantly.

ACKNOWLEDGMENTS

The author would like to thank Dr. N. Nakhjiri for helpful discussion and A. Lewis for development of visualization tools.

REFERENCES

1. K. Autumn, MRS Bull. **32(6)**, 473 (2007); doi: 10.1557/mrs2007.80.
2. K. Autumn, P.H. Niewiarowski, and J.B. Puthoff, Ann. Rev. Ecol. Evol. Syst. **45**, 445 (2014); doi: 10.1146/annurev-ecolsys-120213-091839.
3. Gravish et al., J. R. Soc. Interface **7(43)**, 259 (2010); doi: 10.1098/rsif.2009.0133.
4. J. Puthoff, et al., Soft Matter **9(19)**, 4855 (2013); doi: 10.1039/c3sm50267h.
5. B.N.J. Persson, Phys. Rev. B **51(19)**, 13568 (1995); doi: 10.1103/physrevb.51.13568.

6. K. Brörmann, I. Barel, M. Urbakh, and R. Bennewitz, *Tribol. Lett.* **50(1)**, 3 (2013); doi: 10.1007/s11249-012-0044-3.